

Adsorption and Desorption Behavior of *n*-Butane and Isobutane on Pt(111) and Sn/Pt(111) Surface Alloys

Chen Xu,[†] Bruce E. Koel,^{*†} and Mark T. Paffett[‡]

Chemistry Department, University of Southern California, Los Angeles, California 90089-0482, and CLS-1, MS G740, Los Alamos National Laboratory, Los Alamos, New Mexico 87545

Received June 2, 1993. In Final Form: October 26, 1993*

The adsorption/desorption behavior of *n*-butane and isobutane on Pt(111) and the p(2×2) Sn/Pt(111) and ($\sqrt{3}\times\sqrt{3}$)R30° Sn/Pt(111) surface alloys has been examined using a combination of adsorption kinetics measurements utilizing a collimated molecular beam and temperature programmed desorption (TPD) mass spectroscopy. Initial sticking probabilities for both molecules on Pt(111) and the surface alloys at temperatures below the monolayer desorption threshold are essentially unity ($S_0 \geq 0.95$). The monolayer saturation coverages of *n*-butane and isobutane were also independent of the amount of Sn in the surface layer. The desorption activation energies measured by TPD for the monolayer states of both *n*-butane and isobutane progressively decrease by 5–8 kJ/mol compared to Pt(111) as the surface concentration of Sn increases from 0.25 to 0.33 atom fraction in the respective surface alloys. The decrease in the desorption activation energy scales linearly with the Sn concentration. No thermal decomposition of either molecule on any surface occurred during TPD measurements. Molecular interactions probed by adsorption and desorption of saturated C₄ hydrocarbons are not influenced as strongly by the presence of Sn in the Pt(111) surface as previously observed for unsaturated molecules, such as ethylene and isobutylene. The rate constants for adsorption and desorption of *n*-butane derived from these ultrahigh vacuum studies are used to help explain the kinetics determined in recent, moderate pressure (50–200 Torr) studies of the hydrogenolysis of *n*-butane over these Sn/Pt(111) surface alloys.

1. Introduction

The surface chemistry of the small paraffins *n*-butane and isobutane on Pt and Pt–Sn alloys is of fundamental interest as it relates to elementary steps in heterogeneous catalysis of hydrocarbon conversion. Supported Pt is well-known to catalyze these reactions, and various metal additives such as Sn are often used in bimetallic Pt catalysts to alter the selectivity in these reactions and to reduce coking.¹ The isomerization of *n*-butane to isobutane is an important reforming reaction in which the antiknock quality of gasoline is improved and is an important reaction to increase the yield in isobutylene production. The catalytic dehydrogenation of isobutane to produce isobutylene is receiving more attention now since isobutylene is used in the production of MTBE, an important additive for gasoline. *n*-Butane and isobutane are reactants or products in this catalysis and additional knowledge about their interactions with Pt and Pt–Sn alloys will aid in the understanding of this chemistry.

Understanding the origins of the catalytic effects observed when using bimetallic catalysts is difficult for conventional high surface area supported catalysts since the production of such materials invariably leads to a multitude of different bimetallic structural features present, e.g., bimetallic clusters, alloys, metal particle edge decoration and reconstructed faces, etc. Recently it has been demonstrated that highly ordered bimetallic surface alloys can be prepared by annealing ultrathin films of Sn vapor deposited on a number of group VIII single crystal substrates.^{2–4} Specifically, it has been shown that both the p(2×2) Sn/Pt(111) and ($\sqrt{3}\times\sqrt{3}$)R30° Sn/Pt(111)

surfaces prepared in this manner are substitutional surface alloys.⁵ Taking advantage of the ability to prepare a relatively large ($\approx 1 \text{ cm}^2$) monolithic surface and to directly compare the reactivity to a Pt(111) single crystal substrate, the reactivity of both of the above-mentioned Sn/Pt(111) surface alloys for *n*-butane hydrogenolysis at moderate pressures (50–200 Torr) over the temperature range 500–675 K has recently been examined.^{6,7} The main features observed were notably different overall activities and selectivities and substantially reduced graphitic carbon buildup (induced catalyst deactivation) on both Sn/Pt(111) surface alloys. The (2×2)Sn/Pt(111) surface alloy was observed to be the most active followed by Pt(111) and then the ($\sqrt{3}\times\sqrt{3}$)R30° Sn/Pt(111) surface alloy. To help clarify the role that the surface–adsorbate interaction plays in this catalytic behavior, we have examined the adsorption and desorption kinetics of *n*-butane and isobutane on Pt(111) and the p(2×2) Sn/Pt(111) and the ($\sqrt{3}\times\sqrt{3}$)R30° Sn/Pt(111) substitutional surface alloys.

2. Experimental Methods

The experiments were performed in a stainless steel ultrahigh vacuum (UHV) chamber. The system was equipped with a double-pass cylindrical mirror analyzer (CMA) for Auger electron spectroscopy (AES), four-grid low energy electron diffraction (LEED) optics, shielded quadrupole mass spectrometer (QMS) for temperature programmed desorption (TPD) mass spectrometry, and a directed molecular beam doser for making sticking coefficient measurements. The system base pressure was 6×10^{-11} Torr. TPD measurements were made using the QMS in line-of-sight with the sample surface and using a linear sample heating rate of 4–5 K s⁻¹.

The Pt(111) single crystal (Atomerig, 5N purity) was cleaned

[†] University of Southern California.

[‡] Los Alamos National Laboratory.

* Abstract published in *Advance ACS Abstracts*, December 15, 1993.

(1) Sinfelt, J. H. In *Catalysis: Science and Technology*; Anderson, J. R., Boudart, M., Eds.; Springer-Verlag, Berlin: 1981; Vol. 1, p 258.

(2) Paffett, M. T.; Windham, R. G. *Surf. Sci.* 1989, 208, 34.

(3) Paffett, M. T.; Logan, A. D.; Simonson, R. J.; Koel, B. E. *Surf. Sci.* 1991, 250, 123.

(4) Paffett, M. T.; Logan, A. D.; Taylor, T. N. *J. Phys. Chem.* 1993, 97, 690.

(5) Overbury, S. H.; Mullins, D. R.; Paffett, M. T.; Koel, B. E. *Surf. Sci.* 1991, 254, 45.

(6) Logan, A. D.; and Paffett, M. T. *Proceedings of the 10th International Conferences on Catalysis*; Akademiai Kiado: Budapest, Hungary, 1992; Vol. B, p 1595.

(7) Logan, A. D.; Henn, F. C.; Anderson, S.; Dartye, A.; Paffett, M. T. Submitted for publication in *J. Catal.*

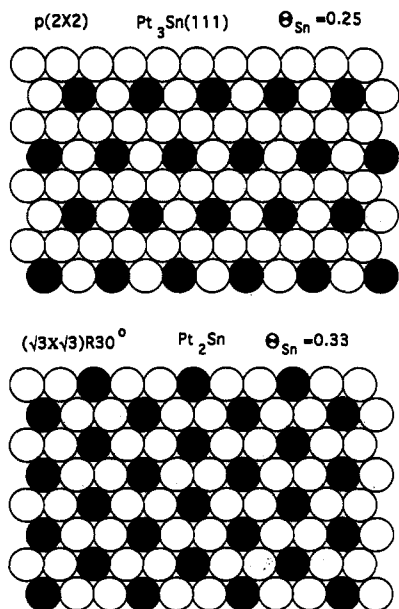


Figure 1. Structures for the $p(2 \times 2)$ and $(\sqrt{3} \times \sqrt{3})R30^\circ$ Sn/Pt(111) surface alloys.

using the procedure found in ref 8. The Pt(111) crystal (10 mm diameter, 1 mm thick) was suspended between two 20-mil Ta wires and could be cooled down to 95 K using liquid nitrogen or resistively heated to 1200 K. The temperature was measured by a chromel–alumel thermocouple spot-welded to the side of the crystal.

n-Butane (Matheson, 99.9%) and isobutane (Matheson, 99.9%) were used as received. Gas exposures were made using leak valves connected to collimated microcapillary array dosers and are given in units of langmuirs ($1 \text{ langmuir} = 10^{-6} \text{ Torr s}$) uncorrected for doser enhancement factor and ion gauge sensitivity. Adsorbate coverages in this paper are referenced to the Pt(111) surface atom density, i.e., $\theta = 1.0$ corresponds to $1.505 \times 10^{15} \text{ atoms cm}^{-2}$.

n-Butane and isobutane absolute sticking coefficients were measured directly using the simple beam reflection method of King and Wells.⁹ Our application of this method has been described previously.^{10,11} The hydrocarbon coverages, θ_{HC} , were calibrated with the following equation

$$\theta_{\text{HC}} = \frac{P_{\text{HC}}}{P_{\text{CO}}} \left(\frac{M_{\text{CO}}}{M_{\text{HC}}} \right)^{1/2} \frac{\int S_{\text{HC}} dt}{\int S_{\text{CO}} dt} \theta_{\text{CO}} \quad (1)$$

using the saturation coverage of CO, $\theta_{\text{CO}} = 0.5$, on clean Pt(111) at 300 K.¹²

The $p(2 \times 2)$ Sn/Pt(111) and $(\sqrt{3} \times \sqrt{3})R30^\circ$ Sn/Pt(111) surface alloys were prepared by evaporating Sn on the clean Pt(111) surface and subsequently annealing the substrate to 1000 K for 10 s. Depending on the initial Sn coverage, the annealed surface exhibited either a $p(2 \times 2)$ or $(\sqrt{3} \times \sqrt{3})R30^\circ$ LEED pattern as previously reported.^{2,5} These LEED patterns are due to substitutional surface alloys corresponding to the (111) face of Pt_3Sn and an ordered hexagonal face of composition of Pt_2Sn as shown in Figure 1. Angle-dependent low energy ion scattering spectroscopy (LEISS) measurements made using 500–1000 eV Li^+ ions have demonstrated that substitutional surface alloys are produced with the Sn atoms nearly coplanar with the Pt surface atoms (0.22 Å outward bucking of the Sn atoms from the surface plane).⁵ For brevity throughout this paper, we will refer to the $p(2 \times 2)$ Sn/Pt(111) and $(\sqrt{3} \times \sqrt{3})R30^\circ$ Sn/Pt(111) surface alloys as the (2×2) and $\sqrt{3}$ alloy surfaces, respectively.

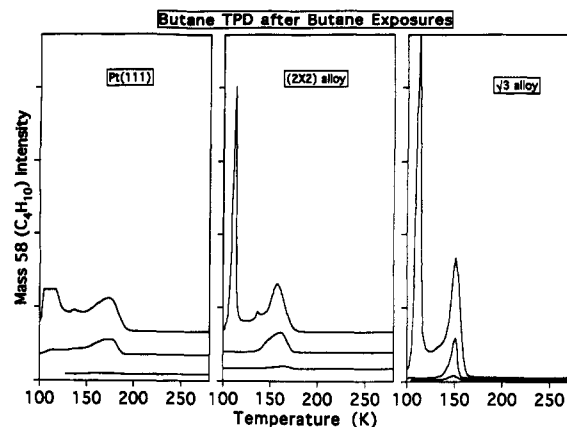


Figure 2. Butane TPD spectra after *n*-butane exposures on the Pt(111) surface, (2×2) Sn/Pt(111) surface alloy, and $(\sqrt{3} \times \sqrt{3})R30^\circ$ Sn/Pt(111) surface alloy. The multilayer desorption peak from the Pt(111) surface at the highest exposure has been artificially cut-off at a small intensity. Exposures from bottom to top were 0.1, 0.4, and 2 langmuirs.

3. Results

3.1. Desorption Energetics Using TPD. A series of TPD spectra of *n*-butane desorption from Pt(111) and the (2×2) and $\sqrt{3}$ alloys are shown in Figure 2. All *n*-butane exposures were given at surface temperatures of 95–110 K and are listed in the figure caption. At low exposures, a rather broad monolayer desorption state of *n*-butane/Pt(111) is observed with a desorption peak temperature of 179 K which is relatively invariant with increasing coverage. Alloying Pt with Sn lowers the desorption temperature for the *n*-butane monolayer to 160 and 153 K for the (2×2) and the $\sqrt{3}$ alloy surfaces, respectively. The TPD peak maxima for these surfaces are also independent of *n*-butane coverage. Analysis of these desorption peak maxima leads to desorption activation energies of 45, 40, and 38 kJ/mol, respectively, assuming a preexponential factor of $1 \times 10^{13} \text{ s}^{-1}$ and first-order desorption kinetics.¹³ A multilayer or condensed phase can be formed at these low temperatures for larger exposures, and the multilayer desorption peak temperature of 112 K for *n*-butane sublimation from all three surfaces is essentially the same for nearly identical exposures. Assuming a preexponential factor of $1 \times 10^{28} \text{ s}^{-1} \text{ cm}^{-2}$ for a zero-order desorption process, the desorption temperature at a *n*-butane coverage of approximately two layers corresponds to a desorption activation energy of 27 kJ/mol for the *n*-butane multilayer phase. An approximate calculation of the heat of sublimation for *n*-butane at this temperature from bulk properties¹⁴ assuming a constant heat capacity gives a similar value of 33 kJ/mol.

Hydrogen evolution from *n*-butane dehydrogenation monitored after dosing sufficient *n*-butane to saturate the monolayer phase was monitored by the H_2 TPD traces provided in Figure 3. For comparison, an H_2 TPD curve following a saturation coverage of adsorbed hydrogen produced by H_2 exposure on Pt(111) is also shown. On all three surfaces, H_2 desorption following *n*-butane exposure is negligible. Estimates of the maximum amount of decomposition using these H_2 TPD peak areas yield values of decomposition less than 1%, which should be attributed probably to contributions from defects (and residual H_2 coadsorption for Pt(111)). Consistent with these TPD

(8) Paffett, M. T.; Campbell, C. T.; Taylor, T. N.; Srinivasan, S. *Surf. Sci.* 1985, 154, 284.

(9) King, D. A.; Wells, M. G. *Surf. Sci.* 1972, 29, 454.

(10) Jiang, L. Q.; Koel, B. E.; Falconer, J. L. *Surf. Sci.* 1992, 273, 273.

(11) Jiang, L. Q.; Koel, B. E. *J. Phys. Chem.* 1992, 96, 8694.

(12) Norton, P. R.; Davies, J. A.; Jackman, T. E. *Surf. Sci.* 1982, 122, L593.

(13) Redhead, P. *Vacuum* 1962, 12, 203.

(14) *Physical Constants of Hydrocarbons C₁ to C₁₀*; ASTM Data Series; Publication DS4A; ASTM: Philadelphia, PA, 1971.

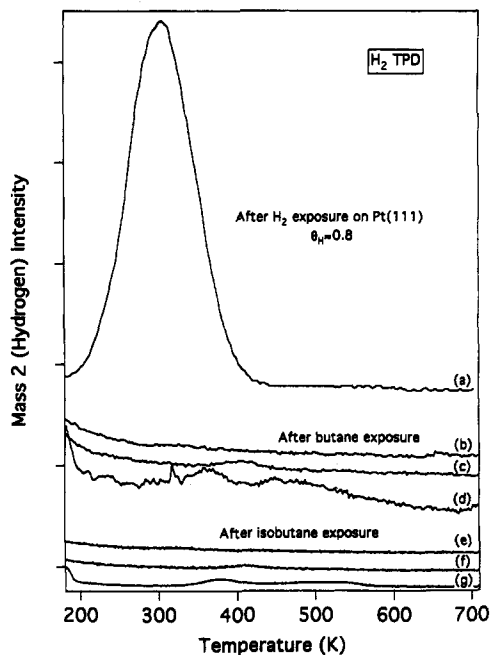


Figure 3. H₂ TPD spectra after (a) saturation exposure of H₂ on Pt(111) at 110 K to give $\theta_{\text{H}} \approx 0.8$, (b–d) large *n*-butane exposures on the $\sqrt{3}$ alloy, (2 \times 2) alloy, and Pt(111) surface at 110 K, respectively, and (e–g) large isobutane exposures on the $\sqrt{3}$ alloy, (2 \times 2) alloy, and Pt(111) surface at 110 K, respectively.

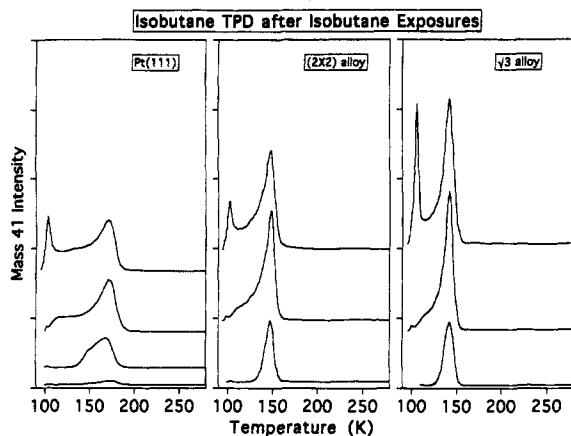


Figure 4. Isobutane TPD spectra after isobutane exposures on the Pt(111) surface, p(2 \times 2)Sn/Pt(111) surface alloy, and the ($\sqrt{3}\times\sqrt{3}$)R30° Sn/Pt(111) surface alloy. Exposures from bottom to top were 0.1, 0.4, and 2 langmuirs.

results, no carbon was detected by AES following each TPD cycle.

In Figure 4, a series of TPD spectra are shown for isobutane desorption following isobutane dosing on Pt(111) and the (2 \times 2) and $\sqrt{3}$ alloys at 95–110 K that are analogous to those in Figure 2. The desorption peak maximum for the monolayer of isobutane on Pt(111) occurs at 179 K with only a limited effect of changing coverage. However, the broadening to lower temperatures near monolayer saturation is more clearly seen in this case, indicating substantial destabilizing effects near saturation coverage in the monolayer. As seen previously for *n*-butane, the isobutane monolayer desorption peak temperature progressively decreases as the surface concentration of Sn increases from 0.25 to 0.33 monolayer in the (2 \times 2) and $\sqrt{3}$ alloys. This peak maximum is observed at 152 and 145 K for the (2 \times 2) and $\sqrt{3}$ alloy, respectively. No noticeable influence of isobutane coverage was observed in the monolayer TPD peak temperatures. These desorption peak maxima translate into activation energies of

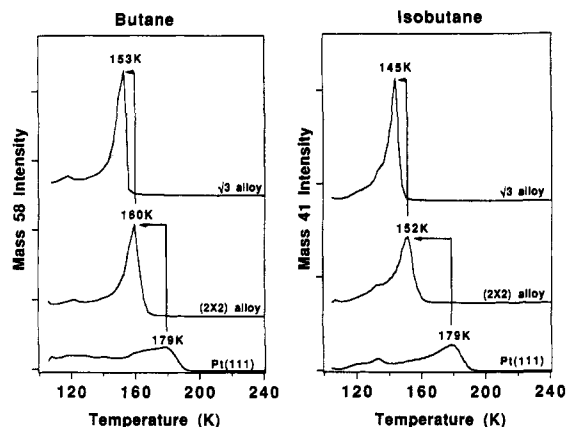


Figure 5. Comparison of *n*-butane and isobutane TPD spectra for monolayer coverages on Pt(111), the p(2 \times 2) surface alloy, and the ($\sqrt{3}\times\sqrt{3}$)R30° Sn/Pt(111) surface alloy.

45, 38, and 36 kJ/mol assuming a preexponential of $1 \times 10^{13} \text{ s}^{-1}$ and a first-order desorption rate process. The isobutane multilayer desorption peak was observed at 105 K on all three surfaces for equivalent exposures. This peak corresponds to an activation energy of about 26 kJ/mol, making the same assumptions stated for *n*-butane above.

Consistent with the *n*-butane interactions described above, the adsorption/desorption behavior of isobutane was observed to be entirely reversible with no evidence of decomposition arising from these limited exposures. In Figure 3, H₂ TPD spectra following isobutane exposures that produce monolayer coverage are shown. An upper limit for the amount of isobutane decomposition to hydrogen and adsorbed carbon is less than 1% of the adsorbed monolayer on any of the three substrates.

In Figure 5 a comparison of the desorption traces for monolayer coverages of *n*-butane and isobutane on Pt(111) and the (2 \times 2) and $\sqrt{3}$ alloys shows clearly the influence of surface Sn in reducing the desorption activation energies to progressively lower values as the surface concentration of Sn increases in the surface alloys.

Figure 6 shows an expanded view of the low temperature region of the isobutane TPD curves for near-monolayer coverages on a number of differently prepared surfaces. The lower three curves are from carefully prepared surfaces with reproducible stoichiometries (by AES) exhibiting clear and sharp LEED patterns. The two alloy surfaces have a uniform composition and geometry as indicated by the schematic drawings in Figure 1. In these cases, and for all but near-monolayer coverages of isobutane on the Sn/Pt(111) surface alloys, isobutane desorbs in a well-defined, narrow peak indicative of a single, well-defined adsorption energy *over the entire surface*. This behavior for the Pt–Sn alloys is notably different from that commonly seen on promoted or poisoned surfaces, such as C₂H₄/K/Pt(111)¹⁵ or C₂H₄/Bi/Pt(111),¹⁶ where one sees an unaltered TPD state due to unmodified sites and sometimes a new TPD state induced by the modifier adatom. We observe a single TPD peak characteristic of each surface alloy. The top two curves in Figure 6 were obtained from defective surfaces containing multiple phases or domains. The surface corresponding to the top-most curve exhibited various LEED patterns as the LEED incident beam was moved across the crystal due to each

(15) Windham, R. G.; Bartram, M. E.; Koel, B. E. *J. Phys. Chem.* 1988, 92, 2862.

(16) Windham, R. G.; Koel, B. E.; Paffett, M. T. *Langmuir* 1988, 4, 1113.

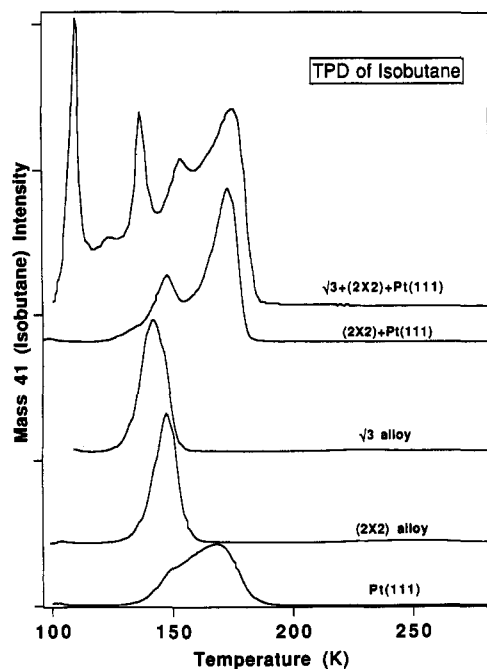


Figure 6. Isobutane TPD spectra for coverages near one monolayer on Pt(111), the p(2×2) surface alloy, and the ($\sqrt{3}\times\sqrt{3}$)R30° Sn/Pt(111) surface alloy, a surface exhibiting a weak p(2×2) LEED pattern, and a surface exhibiting weak spots due to combined p(2×2) and ($\sqrt{3}\times\sqrt{3}$)R30° LEED patterns. The top two curves have different exposures and arbitrary intensities compared to the bottom curves, and the topmost curve shows a low temperature peak characteristic of a small amount of a multilayer isobutane phase.

of the p(2×2) and ($\sqrt{3}\times\sqrt{3}$)R30° domains of alloy phases and Pt(111) domains. Similarly, the second curve from the top was from a sample exhibiting a combination of p(2×2) Sn/Pt(111) surface alloy and Pt(111) domains. With high correlation, isobutane TPD confirms the presence of each phase. The isobutane desorption temperature from each phase is relatively unaffected by the long range order or the defects that are obviously introduced by the domain boundaries.

3.2. Adsorption Kinetics Results. The kinetics of adsorption of the both hydrocarbon molecules were examined on all three surfaces as a function of substrate temperature over the range 95–150 K. A representative set of curves for the *n*-butane sticking coefficient versus coverage are shown in Figure 7 for adsorption on the $\sqrt{3}$ alloy at a variety of surface temperatures. The initial sticking coefficient, S_0 , of *n*-butane is essentially unity ($S_0 \geq 0.95$) independent of the surface temperature over the range of 95–140 K. (The small dip in S at very low coverages is an artifact of the experiment.¹⁰) Under conditions that a multilayer or solid phase is thermodynamically stable ($T \leq 100$ K), the sticking (condensation) coefficient does not diminish with increasing coverage and the coverage on the surface does not saturate. At 125 K, the multilayer phase is not stable and only a monolayer can be formed. Thus, S decreases to zero near $\theta_{\text{isobutane}} = 0.25$ which is the monolayer saturation coverage. The fact that S is independent of isobutane coverage up to about 30% of the saturation coverage usually indicates the importance of a more weakly bound precursor in the adsorption kinetics. A decrease in sticking probability with increasing sample temperature occurs at least in part because of the increasing desorption probability at elevated temperatures ($T \geq 140$ K). The sticking coefficient that we measure at higher temperatures is therefore no longer a true sticking coefficient but rather an apparent sticking

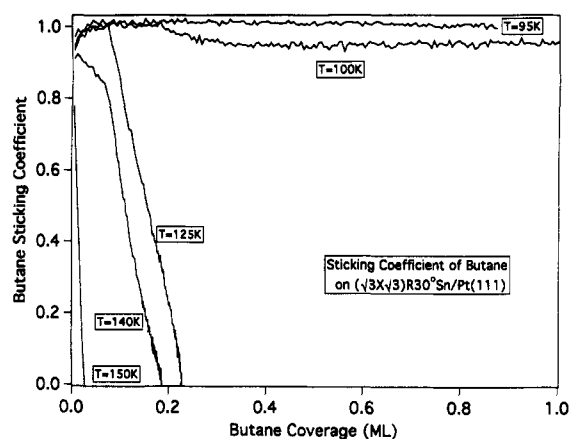


Figure 7. Sticking coefficient of *n*-butane on the ($\sqrt{3}\times\sqrt{3}$)R30° Sn/Pt(111) surface alloy at several different substrate temperatures.

coefficient that is determined by the sum of the true sticking coefficient and the desorption rate.

Identical curves were obtained for *n*-butane adsorption on the (2×2) alloy and on Pt(111) at 95 K. For substrate temperatures of 125 K, where the multilayer is not formed, the same sticking coefficient versus *n*-butane coverage curves were obtained within experimental error: *the sticking coefficient, the role of the precursor, and the monolayer saturation coverage are independent of the amount of Sn in the surface layer.* This behavior is shown in Figure 8. Small differences occur in the saturation coverages measured partly because of the normal experimental uncertainties but also because the adsorption energetics vary somewhat for the three surfaces and we chose a constant adsorption temperature of 125 K for all three surfaces.

An identical series of experiments to those described for Figure 8 were also performed using isobutane on the same three surfaces. The results of these measurements are provided in Figure 9. The sticking probability as a function of isobutane coverage curves are the same within experimental error on all three surfaces for an adsorption surface temperature of 125 K.

The value of $S = 1$ for condensation of *n*-butane and isobutane into the multilayer phase is consistent with the same values determined for cyclohexane¹⁷ and many other hydrocarbon molecules.¹¹

4. Discussion

The adsorption of *n*-butane and isobutane has been studied previously on several transition metal surfaces, for example, Pt(111),^{18,19} Ni(100),²⁰ Pt(110)-(1×2),²¹ Mo(100),²² and Ir(110)-(1×2).²³ Except for Pt(111) and Ni(100), all of the surfaces mentioned above display some reactivity toward *n*-butane and isobutane decomposition. On Mo(100), less than 5% decomposes following thermal desorption of a *n*-butane monolayer.²² Essentially complete decomposition is observed on Pt and Ir (110)-(1×2) surfaces at small initial coverages.^{21,23} However, the adsorption of *n*-butane and isobutane on Pt(111) is

(17) Xu, C.; Tsai, Y.-L.; Koel, B. E. *J. Phys. Chem.* 1994, 98, 585.

(18) Salmeron, M.; Somorjai, G. A. *J. Phys. Chem.* 1981, 85, 3835.

(19) Chesters, M. A.; Gardner, P.; McCash, E. M. *Surf. Sci.* 1989, 209, 89.

(20) Hamza, A. V.; Madix, R. J. *Surf. Sci.* 1987, 179, 25.

(21) Szuromi, P. D.; Engstrom, J. R.; Weinberg, W. H. *J. Phys. Chem.* 1985, 89, 2497.

(22) Kelly, D. G.; Salmeron, M.; Somorjai, G. A. *Surf. Sci.* 1986, 175, 465.

(23) Szuromi, P. D.; Weinberg, W. H. *Surf. Sci.* 1985, 149, 226.

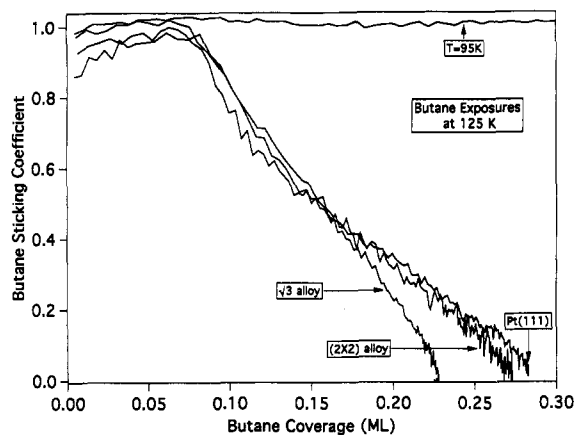


Figure 8. Sticking coefficient of *n*-butane on Pt(111), the p(2×2)-Sn/Pt(111) surface alloy, and the ($\sqrt{3}\times\sqrt{3}$)R30° Sn/Pt(111) surface alloy.

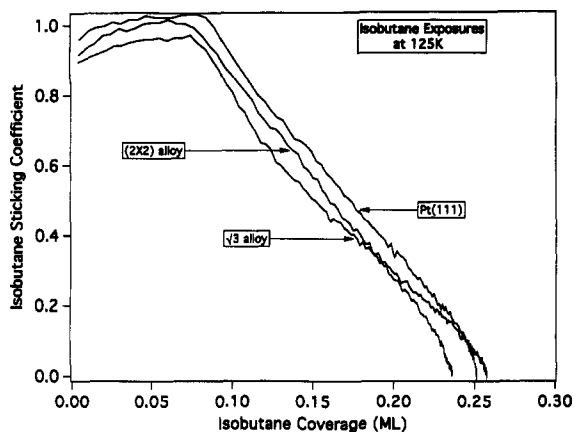


Figure 9. Sticking coefficient of isobutane on Pt(111), the p(2×2)Sn/Pt(111) surface alloy, and the ($\sqrt{3}\times\sqrt{3}$)R30° Sn/Pt(111) surface alloy.

completely reversible, as previously shown by Somorjai and co-workers.¹⁸ Further work by Chesters et al.¹⁹ using infrared measurements was interpreted in terms of a preference by *n*-butane for an adsorption geometry lying flat on the surface with the hydrocarbon backbone parallel to the surface plane. In behavior similar to that seen previously,¹⁸ we find that *n*-butane and isobutane desorb reversibly from Pt(111) in two states: a multilayer or condensed phase at about 105–112 K and a monolayer phase at 179 K for both *n*-butane and isobutane. The desorption activation energies corresponding to these peaks are equal to the adsorption energies, since molecular adsorption is not activated. Analysis of our TPD data gives a sublimation energy of 26–27 kJ/mol and an adsorption energy of 45 kJ/mol for both molecules on Pt(111). No decomposition was ever detected in any of our TPD experiments.

The presence of Sn in the surface layer of the substitutional Sn/Pt(111) surface alloys decreases the binding energy of the saturated C₄ molecules *n*-butane and isobutane by approximately 10% in comparison to Pt(111). The decrease in the TPD peak temperatures is slightly larger for isobutane than for *n*-butane on both Sn/Pt(111) surface alloys. These observations indicate an important electronic influence of Sn on the adsorption energetics of *n*-butane and isobutane on the two substitution surface alloys leading to slightly weaker adsorbate-surface bonding. We have seen similar effects for cyclohexane,¹⁷ methylcyclohexane, and other alkane desorption from these Sn/Pt(111) surface alloys, and a small linear decrease in the adsorption energy always occurs with a

very similar slope with increasing Sn concentration. Additionally, the observations shown in Figure 6 yield two important conclusions. First, the ordered Sn/Pt(111) alloy surfaces that we prepare and use to elucidate the chemistry at Pt–Sn alloy surfaces are uniform and have few defects beyond those inherent to normal single crystals of metals. Secondly, the Sn/Pt(111) surface alloys adsorb and desorb *n*-butane and isobutane with a single, well-defined binding energy; *n*-butane and isobutane do not distinguish between Sn and Pt sites.

Previous TPD results²⁴ for ethylene (C₂H₄) adsorption on these same two Sn/Pt(111) substitutional surface alloys indicated a much more pronounced effect of Sn in decreasing the surface-adsorbate bond strength. Alloying caused nearly a 40% decrease in the ethylene desorption activation energy on the $\sqrt{3}$ alloy compared to Pt(111). This effect was expected because the substantial electronic interactions that occur during alloying Sn with Pt should influence the rehybridized, di- σ -bonded ethylene molecule (and other olefins and arenes) more strongly than the weak bonding of saturated hydrocarbons (paraffins) such as *n*-butane and isobutane.

In contrast to the important effects of surface Sn on the adsorption energetics, the sticking coefficients and saturation coverages of *n*-butane and isobutane were not affected by the presence of Sn. Even though Sn has been referred to as an inert site-blocking component in discussing the hydrocarbon conversion chemistry that occurs on Pt–Sn bimetallic catalysts, our results show that Sn has *no site blocking effect* on the initial elementary steps of catalysis involving the adsorption of *n*-butane and isobutane on Sn/Pt(111) surface alloys. Attempts to model catalytic reactions using expressions such as $(1 - n\theta_{\text{Sn}})^m$ in rate expressions for reactant adsorption and in expressions for available surface sites for adsorption would be incorrect.

The hydrogenolysis and isomerization of *n*-butane at moderate pressures (0.1–200 Torr) have been extensively studied on supported Pt,^{25,26} Pt single crystals,²⁷ and Sn/Pt(111) surface alloys.^{5,6} Davis et al.²⁷ saw substantial isomerization activity in studies of the hydrogenolysis of *n*-butane over Pt(111) model catalysts. However, later work by Logan et al.^{6,7} observed much lower isomerization activity. Focusing on the hydrogenolysis activity, Pt(111) was more active by a factor of ≈ 8 over the temperature range 525–675 K when compared to the ($\sqrt{3}\times\sqrt{3}$)R30° Sn/Pt(111) surface alloy. The (2×2) surface alloy was, however, approximately a factor of 5 higher in overall activity over the temperature range 530–610 K. For all three surfaces, Arrhenius behavior was obtained for hydrogen to *n*-butane ratios of 20:1 with the same observed apparent activation energies of 115 kJ/mol. The specific activity (turnover frequency or TOF) of Pt(111) at 600 K under these conditions was 0.1 molecule site⁻¹ s⁻¹. From the kinetic theory of gases the collision frequency of *n*-butane molecules with the Pt surface follows from

$$Z = (3.513 \times 10^{22})[P/\sqrt{MT}] \quad (2)$$

where *P* is the gas pressure in Torr, *M* is the molecular weight of the molecule, and *T* is the temperature of the gas molecules. The appropriate gas temperature is the

(24) Paffett, M. T.; Gebhard, S.; Windham, R. G.; Koel, B. E. *Surf. Sci.* 1989, 223, 449.

(25) Bond, G. C. *Proceedings of the 10th International Conference on Catalysis*; Akademiai Kiado: Budapest, Hungary, 1992; Vol. A, p 849.

(26) Anderson, S.; Datsy, A. University of New Mexico, private communication.

(27) Davis, S. M.; Zaera, F.; Somorjai, G. A. *J. Am. Chem. Soc.* 1982, 104, 7453.

substrate temperature for the reactor of reference [6,7] because the mean free path of the hydrocarbon molecules at 10 Torr is sufficiently small that a stagnant diffusion layer is formed near the catalyst surface. At 600 K the collision frequency for *n*-butane is 1.25×10^6 molecules $\text{site}^{-1} \text{s}^{-1}$ for Pt(111), which yields a reaction probability of 8×10^{-8} at 600 K and 10 Torr partial pressure of *n*-butane. The reaction probability is decreased by almost another order of magnitude on the $\sqrt{3}$ alloy surface. Clearly the close-packed Pt(111) surface is extremely unreactive for this catalysis and a further decrease occurs in the specific activity over the Sn/Pt(111) surface alloys.

In explaining the reduction in activity for the Sn/Pt(111) alloy compared to Pt(111), one must remember that the *n*-butane molecular sticking coefficient and the saturation coverage for molecular adsorption are not affected by Sn. However, the adsorption energetics are altered on the Pt-Sn alloy. If one carries out a calculation of the reduction in the equilibrium coverage of *n*-butane on the Pt-Sn alloy due to the reduction in the heat of adsorption compared to Pt(111), as measured by our experiments reported herein, one obtains a factor of 4.²⁸ To obtain a factor of 8 requires a difference in the heats of adsorption of about 10 kJ/mol rather than the 7 kJ/mol that we measured. This is probably within our experimental error, but it is certainly possible that changes in other elementary steps are important as well. For example, if the initial C-H bond-breaking step were rate-limiting for the overall reaction, then a concomitant small change in the activation energy of this step would be required to balance the change in *n*-butane adsorption energy to maintain a constant apparent activation energy for the two surfaces. Very similar influences of Sn on activity have been observed over the $(\sqrt{3} \times \sqrt{3})R30^\circ$ Sn/Ni(111) and $(\sqrt{3} \times \sqrt{3})R30^\circ$ Sn/Rh(111) surface alloys,⁶ and it is plausible that such a simple explanation can account for these differences as well.

The catalytic selectivities observed over Pt(111), the $(2 \times 2)\text{Sn/Pt}(111)$ surface alloy, and $(\sqrt{3} \times \sqrt{3})R30^\circ$ Sn/Pt(111) surface alloy indicate some additional differences in the surface chemistry. Hydrogenolysis of *n*-butane on Pt(111) over the temperature range 530–610 K produces a relatively invariant selectivity (mole %) of 47–51% CH_4 , 28–34% C_2H_6 , and 16–20% C_3H_8 , with less than 1% isobutane.⁵ Similar selectivities were observed at the $(\sqrt{3} \times \sqrt{3})R30^\circ$ Sn/Pt(111) surface alloy. However, the $(2 \times 2)\text{Sn/Pt}(111)$ surface alloy gave selectivities over the same temperature range ranging from 22 to 50% for CH_4 , 50 to 40% for C_2H_6 , 25 to 10% for C_3H_8 , and <1% for isobutane. The minor relative differences between the adsorption energetics of *n*-butane and isobutane on these three surface cannot account for the selectivity differences. A more plausible explanation is that there is an altered stability of intermediates on the two Sn/Pt(111) surface alloys compared to the Pt(111) surface. For example, we have observed large reductions in the heats of adsorption of olefins such as ethylene²⁴ and isobutylene²⁹ and even larger changes in the dehydrogenation activity²⁴ and reactivity³⁰ of these Pt-Sn alloy surfaces.

Acknowledgment. This work was supported by the U.S. Department of Energy, Office of Basic Energy Sciences, Chemical Sciences Division.

(28) The kinetic data were obtained in a regime where the surface coverage was significantly less than 1. A simple calculation shows only about 1×10^{-3} monolayer to be present on the surface under the conditions used in the kinetic experiments. The equilibrium coverage can be calculated using $\theta = (Z/\nu) * e^{E/RT}$, where Z is the collision frequency of the gas molecules and ν and E are the preexponential factor and the desorption activation energy, respectively, for the molecule on the surface. For 600 K and 10 Torr, this calculation yields 0.001 monolayer.

(29) Xu, C.; Paffett, M. T.; Koel, B. E. To be submitted for publication.

(30) Xu, C.; Peck, J. W.; Koel, B. E. *J. Am. Chem. Soc.* **1993**, *115*, 751.